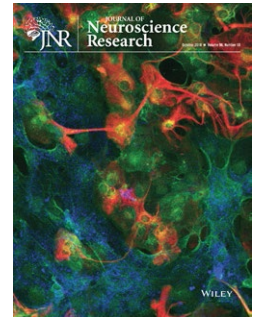


## RESEARCH ARTICLE

# Downregulation of tyrosine hydroxylase phenotype after AAV injection above substantia nigra: Caution in experimental models of Parkinson's disease



Katrina Albert<sup>1</sup>  | Merja H. Voutilainen<sup>1</sup> | Andrii Domanskyi<sup>1</sup> |  
 T. Petteri Piepponen<sup>2</sup> | Sari Ahola<sup>1</sup> | Raimo K. Tuominen<sup>2</sup> |  
 Christopher Richie<sup>3</sup> | Brandon K. Harvey<sup>3</sup> | Mikko Airavaara<sup>1</sup> 

<sup>1</sup>Institute of Biotechnology, Program of Developmental Biology, University of Helsinki, Helsinki, Finland

<sup>2</sup>Division of Pharmacology and Pharmacotherapy, University of Helsinki, Helsinki, Finland

<sup>3</sup>Intramural Research Program, National Institute on Drug Abuse, NIH, Baltimore, Maryland

## Correspondence

Mikko Airavaara, Institute of Biotechnology, Program of Developmental Biology, University of Helsinki, Helsinki, Finland.  
 Email: mikko.airavaara@helsinki.fi

## Abstract

Adeno-associated virus (AAV) vector-mediated delivery of human  $\alpha$ -synuclein ( $\alpha$ -syn) gene in rat substantia nigra (SN) results in increased expression of  $\alpha$ -syn protein in the SN and striatum which can progressively degenerate dopaminergic neurons. Therefore, this model is thought to recapitulate the neurodegeneration in Parkinson's disease. Here, using AAV to deliver  $\alpha$ -syn above the SN in male and female rats resulted in clear expression of human  $\alpha$ -syn in the SN and striatum. The protein was associated with moderate behavioral deficits and some loss of tyrosine hydroxylase (TH) in the nigrostriatal areas. However, the immunohistochemistry results were highly variable and showed little to no correlation with behavior and the amount of  $\alpha$ -syn present. Expression of green fluorescent protein (GFP) was used as a control to monitor gene delivery and expression efficacy. AAV-GFP resulted in a similar or greater TH loss compared to AAV- $\alpha$ -syn and therefore an additional vector that does not express a protein was tested. Vectors with double-floxed inverse open reading frame (DIO ORF) encoding fluorescent proteins that generate RNA that is not translated also resulted in TH downregulation in the SN but showed no significant behavioral deficits. These results demonstrate that although expression of wild-type human  $\alpha$ -syn can cause neurodegeneration, the variability and lack of correlation with outcome measures are drawbacks with the model. Furthermore, design and control selection should be considered carefully because of conflicting conclusions due to AAV downregulation of TH, and we recommend caution with having highly regulated TH as the only marker for the dopamine system.

## KEYWORDS

adeno-associated virus, alpha-synuclein, DIO, dopamine, GFP, Parkinson's disease, substantia nigra

**Significance**

We performed experiments injecting adeno-associated virus (AAV)- $\alpha$ -synuclein and four different control vectors in rats. All vectors decreased nigral TH<sup>+</sup> cell number without a significant loss of nigral neurons, nor striatal dopamine neurites. Additionally, green fluorescent protein (GFP) causes similar TH downregulation equal to or greater than  $\alpha$ -synuclein overexpression. We demonstrate that this is not an ideal model for testing therapies and our results are useful for those who would set up the model. We recommend an AAV control vector that produces protein localized similarly to  $\alpha$ -synuclein in neurons and to consider that downregulation of TH does not always reflect neurodegeneration.

**1 | INTRODUCTION**

Parkinson's disease is a neurodegenerative disorder characterized by its cardinal motor symptoms (tremor, rigidity, bradykinesia, and postural instability), the severity of which correlates with the degeneration of dopamine neurons of the substantia nigra (Cheng, Ulane, & Burke, 2010); non-motor symptoms such as gastrointestinal, olfactory, and sleep disturbances as well as Lewy bodies also characterize the disease. Lewy bodies observed in the *postmortem* analyses of the brain (Spillantini et al., 1997) contain fibrillary forms of  $\alpha$ -synuclein ( $\alpha$ -syn) as well as other proteins, and have been observed to spread to dopamine neurons in the substantia nigra (Braak et al., 2003). The role of  $\alpha$ -syn in disease progression is not clear, but it has been observed that  $\alpha$ -syn, a physiologically pre-synaptic SNARE complex protein (Burre et al., 2010), is found in dopamine neurons of the substantia nigra of healthy aged controls and Parkinson's disease patients. Furthermore,  $\alpha$ -syn density in dopamine neurons is tied to a loss of tyrosine hydroxylase (TH), the rate-limiting enzyme in dopamine synthesis (Chu & Kordower, 2007). These findings have inspired research in developing animal models to reveal the mechanism of  $\alpha$ -syn's possible neurotoxic effect.

Though genetic models of the disease have proven valuable (Blesa & Przedborski, 2014), models that attempt to replicate the more common sporadic form are also necessary. Since  $\alpha$ -syn-containing Lewy bodies are found in all Parkinson's disease patients' *postmortem* brains, one way to model the disease is by overexpressing human wild-type or mutated  $\alpha$ -syn via an adeno-associated virus (AAV) vector. Previous work with AAV- $\alpha$ -syn expression in rats has shown that both changes in behavior and dopamine neuron degeneration are clearly detectable, but milder than the degeneration induced by the toxin 6-hydroxydopamine (6-OHDA) lesion, often used to model Parkinson's disease in animals (Decressac, Mattsson, & Bjorklund, 2012). The same study also found a correlation between motor deficits and dopamine degeneration in rats with  $\alpha$ -syn

overexpression (Decressac, Mattsson, & Bjorklund, 2012). On the other hand, there have been several subsequent studies with AAV- $\alpha$ -syn demonstrating much smaller dopamine deficits, however, these studies did not show whether the biochemical deficits correlated with behavioral deficits (Albert, Voutilainen, Domanskyi, & Airavaara, 2017). Additionally, the results have not always been compared to a control vector (Gaugler et al., 2012) and there have been concerns with overexpression of foreign protein, green fluorescent protein (GFP) in particular, as a control (Andersen et al., 2018; Landeck, Buck, & Kirik, 2016).

We set out to model Parkinson's disease in rats using AAV to express human wild-type  $\alpha$ -syn in substantia nigra in order to recapitulate the dopamine degeneration and motor deficits observed previously and with the intent to test new therapeutics. From our studies, it is clear that there is high variability in the loss of TH in this model. This did not correlate with the typical motor tests used in rat Parkinson's disease models. We also found that the amount of  $\alpha$ -syn present did not correlate with levels of TH. Surprisingly, we found that GFP caused similar TH downregulation to  $\alpha$ -syn. When we switched to AAV-DIO-mCherry as a control, a vector that causes overexpression of RNA, but not of the protein in the absence of Cre recombinase, we found that this resulted in less toxicity and no behavioral deficits compared to AAV- $\alpha$ -syn. This demonstrates that careful consideration needs to be taken when selecting the proper control for these studies.

**2 | MATERIALS AND METHODS****2.1 | Animals**

Seventy-nine young adult male Wistar rats (starting weight 250–300 g) or 79 young female Sprague Dawley rats (starting weight 220–260 g) (Harlan) were followed for 8 weeks after AAV injections. Male Wistar rats were used for the AAV5 experiments, and female Sprague Dawley rats were used for all other experiments. Rats were housed in groups of two to four per cage, under a 12-hr light/dark cycle, with ad libitum access to food and water. All surgeries and behavioral assays were carried out at the University of Helsinki Laboratory Animal Centre facilities. All animal experiments were approved by the Finnish National Board of Animal Experiments and were carried out according to the European Community guidelines for the use of experimental animals. License number ESAVI/7812/04.10.07/2015. All guidelines for reporting the use of the animals were followed and 3R principles were adhered to. All rats had a unique code that did not indicate treatment. Animals were placed into random treatment groups, and experimenter was blind to the treatments at the time of tests and analysis.

**2.2 | Viral vectors**

AAV2-human-wild-type- $\alpha$ -syn ( $1.0 \times 10^{13}$  vg/ml), AAV5-human-wild-type- $\alpha$ -syn ( $1.5 \times 10^{13}$  vg/ml), AAV2-eGFP ( $8.1 \times 10^{12}$  vg/ml), AAV5-eGFP ( $9.5 \times 10^{12}$  vg/ml) with chicken  $\beta$ -actin promoter were

obtained from the Vector Core at the University of North Carolina (Chapel Hill). AAV2-DIO-mCherry ( $3.2 \times 10^{12}$  vg/ml) and AAV5-DIO-mCherry ( $3.3 \times 10^{12}$  vg/ml) were also obtained from the Vector Core at the University of North Carolina (Chapel Hill). AAV1-DIO-iRFP ( $4.39 \times 10^{12}$  vg/ml) was packaged as serotype 1 (Howard, Powers, Wang, & Harvey, 2008), purified and titered at the Optogenetics and Transgenic Technology Core, NIDA IRP, NIH, Baltimore, MD USA as described (Henderson, Wires, Trychta, Richie, & Harvey, 2014). DIO vectors are Cre-dependent vectors, and will not produce protein unless Cre recombinase is present. Since the animals used are wild-type and there is no Cre recombinase present, the vectors should not produce any protein in any of the *in vivo* experiments. AAV1-bGHpA-lacZ-DIO-iRFP ( $2.8 \times 10^{12}$  vg/ml) was made and provided by the Genetic Engineering and Viral Vector Core (GEVVC) at NIDA, NIH, Baltimore, MD USA. Empty vectors are challenging to make so we made AAV1-bGHpA-lacZ-DIO-iRFP, and this vector contains an inactive promoter that is a similar length to the promoter in AAV1-DIO-iRFP. This vector is to control for the effects of an antiviral response. We also tested AAV5-GFP ( $6.6 \times 10^{13}$  vg/ml) with chicken  $\beta$ -actin promoter gifted from Professor Deniz Kirik, Lund University. pAAV EF1a DIO iRFP (pOTTC374) plasmid is available at Addgene (plasmid # 47626). For AAV- $\alpha$ -syn injections, we used a 1:1 mixture of AAV2/2- $\alpha$ -syn and AAV2/5- $\alpha$ -syn, which we further refer to as AAV- $\alpha$ -syn for ease of reading. The same type of mixture was used for both the AAV-eGFP and AAV-DIO-mCherry. The mixture of viruses was used to incur the advantage of both serotypes since the serotypes use different receptors for cell entry, and are also spreading differently in the brain (Davidson et al., 2000).

### 2.3 | Testing AAV1 vectors *in vitro*

HEK-293 (human embryonic kidney) cells (obtained from Xiao Xiao, UNC) were grown in DMEM-HG (Invitrogen) containing 5% bovine growth serum, (BGS; HyClone, Logan, UT) and 1% penicillin-streptomycin as described previously (Howard et al., 2008). HEK293 cells appear homogenous in morphology and are negative for mycoplasma. Cells were transfected using Lipofectamine3000 with pAAV bGHpA lacZ DIO iRFP hGHpA (promoter null control), pAAV EF1a DIO iRFP, and pAAV EF1a iCre according to the manufacturer's protocol. Media was changed on DIV1 and cells were fixed with 4% paraformaldehyde on DIV2. Fluorescent protein expression was detected using an EVOS FL Auto 2 cell imaging station using the Cy5.5 filter (Thermo).

### 2.4 | Stereotaxic injections

All stereotaxic injections were performed under isoflurane anesthesia (4.5% for induction, and 2%–3% for maintenance). Animals were placed in a stereotaxic frame (Stoelting, IL, USA), lidocaine (Orion Pharma, Finland, >0.1 ml) was applied under the skin on top of the head to anesthetize the area and stem bleeding, and a small incision was made to expose the skull. Burr holes in the skull were made unilaterally with a micro-drill. A pulled and coated (Sigmacote®, SL2,

Sigma-Aldrich) glass capillary attached to a 10- $\mu$ l Hamilton syringe (701 N, Hamilton Bonaduz AG) or a 33G steel needle with a 10- $\mu$ l syringe (Nanofil, World Precision Instruments) was used to inject the virus. AAVs were injected either into one site above substantia nigra in Wistar rats or into two sites above the left substantia nigra in Sprague Dawley rats, coordinates from bregma (A/P -5.3; M/L + 2.0; D/V -7.2, or A/P -5.3/-6.0; M/L + 2.0; D/V -7.2, respectively). For single-site injections, a volume of 4  $\mu$ l and a flow rate of 0.1  $\mu$ l/min was used. For the two-site injections, volume was 2  $\mu$ l in each site with a flow rate of 0.5  $\mu$ l/min using an automatic injector (Stoelting, IL, USA) or manually controlled flow rate. The needle was kept in place for 5 min after the injection to minimize backflow. For the separate 6-OHDA experiment, 6-OHDA hydrochloride powder (Sigma-Aldrich, H4381) was dissolved in saline with 0.02% ascorbic acid. For the injections, rats were given desipramine immediately prior to the surgery. The rats were anesthetized and placed in a stereotaxic frame as above and a 26-G steel needle attached to a 10  $\mu$ l Hamilton syringe (701 N, Hamilton Bonaduz AG) was used to inject 6-OHDA into two places in the striatum: coordinates relative to bregma of A/P + 1.6, M/L + 2.2 D/V -5.5 and A/P -0.4, M/L + 3.5, D/V -5.5 from the dura). A total of 20  $\mu$ g was injected, split into the two sites, so that 2.5  $\mu$ l of 4  $\mu$ g/ $\mu$ l 6-OHDA were injected into each site with a flow rate of 0.5  $\mu$ l/min. The needle was kept in place for 5 min. After the surgery, all rats received carprofen for pain relief (Rimadyl, Pfizer, s.c. 5 mg/kg). Rats were placed in a separate recovery cage until awake, then returned to their home cage.

### 2.5 | Cylinder test

Cylinder test was performed similarly to (Schallert, Fleming, Leasure, Tillerson, & Bland, 2000). Rats were placed in a plexiglass cylinder that was elevated on a transparent platform. A camera attached to a computer recorded each rat from underneath the platform. Rats were recorded for 10 min in the cylinder and the analysis was made by an experimenter blind to the treatments. Touches to the wall of the cylinder by ipsilateral paw alone, contralateral paw alone, or both paws were counted. A naïve rat is expected to use both left and right paws approximately 50% of the time. All rats had at least 20 touches on the cylinder wall. The cylinder test was performed at 4 and 8 weeks after AAV injections, all results are from 8 weeks post-AAV injection.

### 2.6 | Amphetamine-induced rotations

Amphetamine-induced rotations were performed as previously (Lindholm et al., 2007). On the day of the test, rats were harnessed, tethered, and placed into large bowls. Rats were allowed to habituate and then a dose of D-amphetamine dissolved in saline was given (Sigma, i.p. 2.5 mg/kg). The device then recorded full 360° turns in both clockwise and counterclockwise directions made by the animal over 120 min using the RotoRat software (Med Associates Inc.). Results are represented as the total ipsilateral turns (toward the injected side) minus the contralateral turns (away from the injected side). Rotations were performed at 8 weeks after AAV injections.

## 2.7 | Immunohistochemistry

Perfusions and stainings were performed similarly to (Penttinen et al., 2016). At the end of each experiment, rats were anesthetized with a high dose of sodium pentobarbital (Orion Pharma, i.p. 90 mg/kg). Rats were perfused intracardially with PBS, and then with 4% paraformaldehyde. The brains were removed and placed in 4% paraformaldehyde overnight, and then transferred to a 20% sucrose solution and stored at +4°C. The brains were frozen in a cryostat (Leica CM3050) and 40- $\mu$ m coronal sections were cut from the start of the striatum to the end (approximately 1.20 to -0.8 mm relative to bregma) and from the start of the midbrain to end of the substantia nigra (approximately -4.4 to -6.72 mm relative to bregma) and were collected in PBS. Every sixth section was collected for immunohistochemistry. They were then transferred to a cryopreservant solution (20% glycerol, 2% DMSO in PBS) and stored at -20°C. For immunostaining, the sections were thawed at room temperature, rinsed with PBS and after blocking of endogenous peroxidase (0.3% H<sub>2</sub>O<sub>2</sub> in PBS) for 30 min, rinsed again and blocked with 4% bovine serum albumin (BSA) and 0.3% Triton X-100 in PBS for 1 hr. Sections were then incubated in the primary antibody (mouse anti-TH monoclonal, Millipore Cat# MAB318, RRID:AB\_2201528, dilution 1:2000; mouse anti-human- $\alpha$ -synuclein Ab-2 (clone syn 211) monoclonal, Lab Vision Cat# MS-1572-P1ABX, RRID:AB\_62624, dilution 1:2000; rabbit anti-GFP polyclonal, Thermo Fisher Scientific Cat# A-11122, RRID:AB\_221569, dilution 1:2000) in BSA blocking buffer overnight at +4°C. After incubation with the primary antibody, sections were rinsed again, and placed in secondary antibody (Vector Laboratories anti-mouse or anti-rabbit biotinylated secondary antibody cat#PK-4002 or PK-4001 dilution 1:200) in BSA blocking buffer for 1 hr at room temperature. After rinsing, sections were incubated in avidin-biotinylated horseradish peroxidase (ABC Kit, Vector Laboratories) in PBS for 1 hr, rinsed, and developed with 0.05% 3,3-diaminobenzidine-4 HCL(DAB) (DAB peroxidase substrate kit, SK-4100, Vector Laboratories) in water for 30–60 s, rinsed with PBS and placed on coated slides. For controls, either the primary or the secondary antibody was omitted. Slides were allowed to dry overnight at room temperature, dehydrated, and mounted with Coverquick 2000 mounting medium.

## 2.8 | Antibody characterization

The TH antibody (mouse anti-TH monoclonal, Millipore Cat# MAB318, RRID:AB\_2201528) recognizes a protein on western blot of 59–61 kDa from mouse brain lysate (manufacturer data sheet) and has shown here a staining pattern in rat brains as observed in (Matlik et al., 2017; Penttinen et al., 2016). The human  $\alpha$ -syn antibody (mouse anti-human- $\alpha$ -synuclein Ab-2 (clone syn 211) monoclonal, Lab Vision Cat# MS-1572-P1ABX, RRID:AB\_62624) recognizes a 14-kDa band in western blot, does not recognize  $\beta$ - or  $\gamma$ -synucleins, recognizes human and not mouse or rat  $\alpha$ -syn (manufacturer data sheet) and (Giasson et al., 2000). The GFP antibody (rabbit anti-GFP polyclonal, Thermo Fisher Scientific Cat# A-11122, RRID:AB\_221569)

recognizes a 32–34-kDa band (manufacturer's data) and shows reactivity after AAV-GFP injections in (Alves et al., 2014).

## 2.9 | Optical density analysis

The optical density of TH+ fibers in the rat striatum was determined using immunostained coronal striatal sections at approximately A/P + 1.7 mm, 0.9 mm, and 0.15 mm relative to bregma. Three sections per animal were analyzed. Slides were scanned with a Panoramic 250 Flash II scanner (3DHISTECH, Budapest, Hungary) at the service provided at the Institute of Biotechnology, University of Helsinki (<http://www.biocenter.helsinki.fi/bi/histoscanner/index.html>). Images were taken with the Panoramic Viewer (3DHISTECH) software, and analyzed using Image-Pro Analyzer 7.0 (Media Cybernetics). Both striatal areas were traced in their entirety to ensure the most accurate results. The contralateral side of each striatal section was used as the control, the corpus callosum was used to eliminate unspecific background staining, and all analyses were done by the experimenter who was blind to the treatments. To obtain the final average optical density per brain, the ipsilateral side, contralateral side, and corpus callosum from one section were measured for the mean intensity (the intensity of pixels divided by the area measured), the corpus callosum mean was subtracted from the mean for each side, and then the ratio of these normalized intensities at ipsilateral/contralateral sides was calculated. The obtained value from each section was then averaged together to obtain the optical density value for each animal; this was calculated as a percent of the contralateral side.

To measure the optical density for  $\alpha$ -syn, a similar method was used as above for TH optical density. Three coronal sections from the striatum at A/P + 1.7 mm, 0.9 mm, and 0.15 mm relative to bregma of each rat that were stained for human  $\alpha$ -syn were used. These were analyzed as above.

## 2.10 | Cell counts

TH+ cells in the substantia nigra pars compacta were counted using MATLAB (R2015a, MathWorks) as described in our recent study (Penttinen et al., 2016). This method has been validated against stereological counting, with a Pearson's  $r$  correlation of 0.925 (Penttinen et al., 2016). In a unilateral 6-OHDA lesion model, this method can be used to get an accurate estimate of the degree of cell loss. Briefly, five to six sections from each brain were used from approximately A/P -4.5 to -6.0 relative to bregma. Pictures were taken using the same method as above in optical density and the algorithm used recognized the TH+ cells based on the staining intensity and size. The background threshold was set manually due to the differences in intensity between immunostainings. This method was performed by an observer who was blind to the treatments and who was trained to recognize TH+ neurons in the SN pars compacta.

To estimate the total number of cells in the substantia nigra pars compacta, we counted the TH+ cells using a technique referred to as convolutional neural network, as in (Penttinen, Parkkinen, Blom,

et al., 2018). Sections were the same as above. The slides were digitized on a whole slide scanner (3DHISTECH) with extended focus which combines several layers of the scanned section into a single focal plane, in this case five layers were scanned at 2- $\mu\text{m}$  intervals for a total of 10  $\mu\text{m}$ . The slides were then uploaded to the Aiforia® platform (Fimmic Oy, Helsinki, Finland) and analyzed using the trained algorithm. The algorithm was trained to recognize TH+ cells by an experimenter trained to recognize TH+ cells in the substantia nigra pars compacta, for more details see (Penttinen, Parkkinen, Blom, et al., 2018). To obtain the final estimated totals, the counts obtained for each section (separated into uninjected and injected sides) were multiplied by 6 since every sixth section was collected during cutting. This method has previously been compared to stereological counting and was found to have Pearson's correlation of  $r = 0.9$  and a difference of less than 1% for estimates of TH+ cells in the substantia nigra pars compacta of rats (Penttinen, Parkkinen, Blom, et al., 2018). Additionally, from the point of view of recognizing the TH+ neurons this is considered to be a less biased method since the sections are analyzed by a computer algorithm. The experimenter was blind to the treatments during tracing of the substantia nigra pars compacta and analysis.

For counting of Nissl+ cells, sections were stained using 0.1% cresyl violet (Santa Cruz, SC-214775). Six sections from the substantia nigra area of each rat were analyzed as above in the MATLAB protocol we have recently established (Penttinen et al., 2016).

## 2.11 | HPLC

Dopamine tissue concentration analysis was carried out as described with small modifications (Airavaara et al., 2006). Briefly, rats were euthanized with  $\text{CO}_2$  and the brain was removed and immediately placed into isopentane on dry ice and then frozen at  $-80^\circ\text{C}$ . The brains were cryo-dissected using a cryostat (Leica CM3050) and tissues were kept frozen at all times. The striatum was dissected and again frozen to use for high-performance liquid chromatography (HPLC). Weighed samples were kept on dry ice, then 500  $\mu\text{l}$  of homogenization solution was added (0.2 M  $\text{HClO}_4$  and antioxidant solution containing oxalic acid with acetic acid and L-cysteine, as in (Kankaanpää, Meririnne, Ariniemi, & Seppala, 2001)) then sonicated at power level 1 2–3 times for 2–3 s, or until no large pieces of tissue were visible in the tube. Samples were kept on ice and then centrifuged at  $4^\circ\text{C}$ , 14,000 rpm for 35 min. Then, 300  $\mu\text{l}$  of supernatant was transferred to 500  $\mu\text{l}$  Vivaspin® filter tubes and centrifuged at  $4^\circ\text{C}$ , 9000 rpm for 35 min. One hundred and twenty microliters of sample were then transferred to HPLC vials. The column (Phenomenex Kinetex 2.6  $\mu\text{m}$ , 4.6  $\times$  50 mm C-18; Phenomenex, Torrance, CA, USA) was kept at  $45^\circ\text{C}$  with a column heater (Croco-Cil, Bordeaux, France). The mobile phase consisted of 0.1 M  $\text{NaH}_2\text{PO}_4$  buffer, 220 mg/L of octane sulfonic acid, methanol (8%), and 450 mg/L EDTA, and the pH was set to 4 using  $\text{H}_3\text{PO}_4$ . A pump (ESA Model 582 Solvent Delivery Module; ESA, Chelmsford, MA) equipped with 2 pulse dampers (SSI LP-21, Scientific Systems, State College, PA) provided 1 ml/min flow rate. Hundred microliters of the sample were

injected into the chromatographic system with a Shimadzu SIL-20AC autoinjector (Shimadzu, Kyoto, Japan). Dopamine was detected using ESA CoulArray Electrode Array Detector, and chromatograms were processed and concentrations of monoamines calculated using CoulArray software (ESA, Chelmsford, MA). Values were calculated as ng/g of wet tissue. Experimenter was blinded to coded animal numbers throughout the analysis.

## 2.12 | Statistical analysis

All statistical calculations performed with SPSS (IBM) and all graphs were made in GraphPad Prism 6 or 7 (GraphPad Software Inc., La Jolla, California, USA). All graphs represented as mean  $\pm$  standard deviation,  $\alpha = 0.05$  was used as the level of significance. Criteria for statistical testing, such as tests that ensure normal distribution of data and equal variances were performed before other statistical tests were used. For data with only two groups and one factor, Student's *t* test was used for statistical analysis. For data with more than two groups and only one factor, one-way analysis of variance (ANOVA) was used. For data with more than two groups and two factors, two-way ANOVA was used. Tukey's or Bonferroni post hoc tests were used in post hoc testing for multiple comparisons in ANOVA, each where appropriate.

## 3 | RESULTS

### 3.1 | Optimization of AAV injections above the substantia nigra of rats

We initiated these studies in Wistar rats using the AAV5- $\alpha$ -syn injection to induce degeneration in dopamine neurons of the substantia nigra. As a negative control, we initially used AAV5-eGFP. Using injection settings where the AAVs were injected into a single site above the substantia nigra with a flow rate of 0.1  $\mu\text{l}/\text{min}$ , GFP expression was found throughout the midbrain and striatum (Figure 1a). With the observation of this indiscriminate overexpression of GFP in the midbrain, we then optimized the injection protocol and found that injecting the AAV vector into two sites above the substantia using a coated glass capillary as described previously (Gombash et al., 2013) resulted in specific expression in the substantia nigra and striatum for both GFP (Figure 1b) and  $\alpha$ -syn (Figure 1c). For the  $\alpha$ -syn, we also combined the vector serotypes AAV2/2 and AAV2/5 (referred to herein as AAV- $\alpha$ -syn) in order to take advantage of both of their cell entry and spreading properties (Davidson et al., 2000). Additionally, we observed that Sprague Dawley rats are more active in rearing behavior in the cylinder test and therefore we conducted experiments on non-drug-induced behavior with this strain of rats. The male Wistar rats we had used for all AAV injections often had 10 rearings or less, making it problematic to obtain accurate results on the cylinder test. Rearing data shown in Figure 1d. ( $n = 79/\text{group}$ , Student's *t* test, two-tailed,  $t = 16.25$ ,  $df = 156$ ,  $p = <0.0001$ ).

In addition to the extensive transgene expression of GFP, we observed TH loss (Figure 1e) and net ipsilateral amphetamine-induced

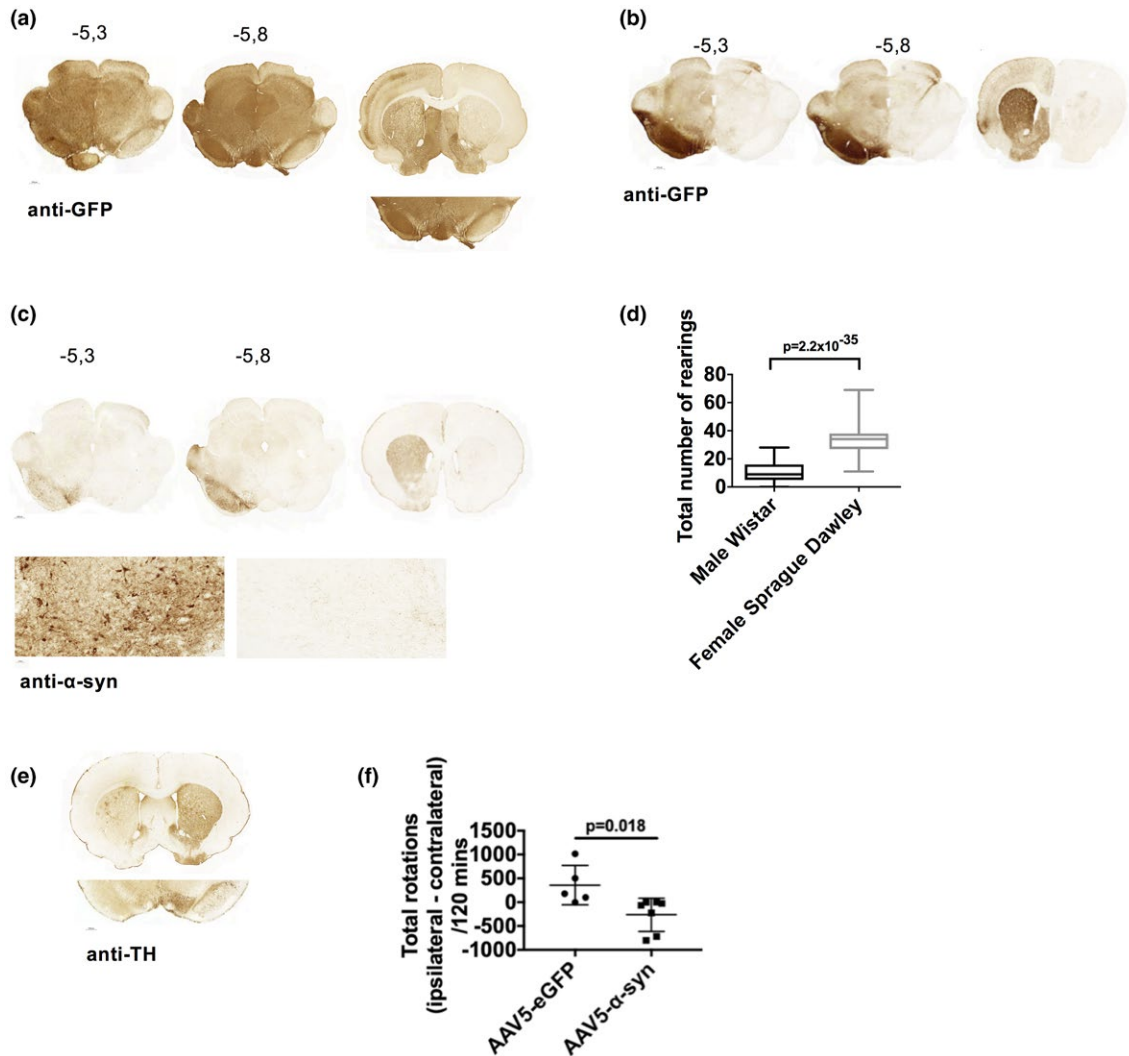


**FIGURE 1** Demonstrating different injection paradigms tested in these experiments and resulting outcomes. (a) Green fluorescent protein (GFP) expression in substantia nigra and striatum using AAV5-eGFP injected above the substantia nigra into one site for male Wistar rats used in the experiments. (b) GFP expression in the substantia nigra and striatum using AAV5-eGFP injected above the substantia nigra into two sites for male Wistar rats used in the experiments. (c) Human  $\alpha$ -synuclein expression in substantia nigra and striatum using AAV- $\alpha$ -synuclein (mixture of AAV2 and AAV5- $\alpha$ -synuclein) injected above the substantia nigra into two sites using male Wistar rats. 40x images of substantia nigra for the injected and uninjected sides are also shown.  $\pm$ SD is used for the error bar of graphs. (d) Number of rearings for Wistar rats ( $n = 79$ ) and Sprague Dawley ( $n = 79$ ) rats used in the experiments. (e) Representative photomicrograph of a male Wistar rat injected with AAV5-eGFP showing tyrosine hydroxylase (TH) immunostaining in the striatum and substantia nigra. (f) Total rotations (ipsilateral-contralateral) on the amphetamine-induced rotational assay (120 min) for AAV5-eGFP ( $n = 5$ ) injected rats and AAV5- $\alpha$ -synuclein ( $n = 7$ ) injected male Wistar rats

rotations in the AAV5-eGFP group (Figure 1f, mean = 358;  $SD = 412.1$ ;  $n = 5$ ) indicating nigrostriatal tract lesions similar in severity to that observed with the 6-OHDA model, where rats may rotate to the ipsilateral side several hundred times in 2 hrs depending on the dose of 6-OHDA (Penttinen et al., 2016). In comparison, AAV5- $\alpha$ -syn injection resulted in contralateral rotations, which differed significantly from the AAV5-eGFP (Figure 1f, Student's  $t$  test, unpaired,  $p = 0.018$ ,  $t = 2.825$ ,  $df = 10$ ,  $n = 5$  for AAV5-eGFP and  $n = 7$  for AAV5- $\alpha$ -syn). Our observed effects of AAV5-eGFP treatment were consistent with data available of the same AAV5-eGFP preparation, where cell loss has also been observed (Michael J. Fox Foundation, 2013).

### 3.2 | Injection of AAV- $\alpha$ -syn above substantia nigra results in high variability on TH loss and causes behavioral deficits inconsistent with mild neurodegeneration

After selecting the injection method, virus serotype, and rat strain for these experiments, we set out to measure the extent of the lesion by analyzing the effects of  $\alpha$ -syn overexpression on the intensity of striatal TH immunoreactivity. In this case, we also chose to mix AAV2/2- $\alpha$ -syn and AAV2/5- $\alpha$ -syn since we saw neurodegeneration with AAV5-eGFP (Figure 1e,f), and wanted to avoid this with GFP. In general, we found that while some rats had clear loss of TH

immunoreactivity, most of the rats clearly did not (Figure 2a, images 1 and 2, Figure 2b). A rat injected with 6-OHDA to the striatum is also shown for comparison to represent total loss of striatal and nigral TH on the ipsilateral side. Although the average TH fiber density was  $61.85\% \pm 30.59\%$  ( $n = 43$ ), the range of results was quite large. Additionally, this TH fiber density did not correlate with the amount of  $\alpha$ -syn present (Figure 2c, Pearson's correlation  $r = 0.1771$ ,  $p = 0.4684$ ,  $n = 19$ ). A summary of results is shown in Table 1. However, there is a small group of rats that had less than 50% TH optical density and low  $\alpha$ -syn optical density. If we remove these on the basis that there is loss of neurites in the striatum, the correlation results are not significantly affected, although they are improved (Pearson's correlation  $r = -0.4855$ ,  $p = 0.0785$ ). The results of only the low TH/low  $\alpha$ -syn do result in a stronger correlation (Pearson's

correlation  $r = 0.7478$ ,  $p = 0.1462$ ). A summary of differential TH optical density loss is shown in Table 2.

Similar variation on TH outcome also occurred in the TH+ cell counts (Figure 2d, mean =  $44.25\% \pm 16.71\%$ ,  $n = 25$ ). While we did observe a moderate behavioral deficit in the cylinder test with ipsilateral paw use being significantly increased compared to contralateral (Figure 2e, one-way ANOVA,  $F(2, 126) = 89.7$ ,  $p < 0.0001$ ,  $n = 43$ ), it did not correlate with TH optical density (Figure 2f, Pearson's correlation  $r = -0.2493$ ,  $p = 0.1313$ ,  $n = 43$ ). As seen from the figure, even the rats that had low TH optical density had little relation to ipsilateral paw use, which is in contrast to the 6-OHDA model. For comparison, the correlation between TH optical density and ipsilateral paw use for the 6-OHDA model in rats is shown (Figure 2g), where there is a clear and strong correlation (Pearson's correlation,

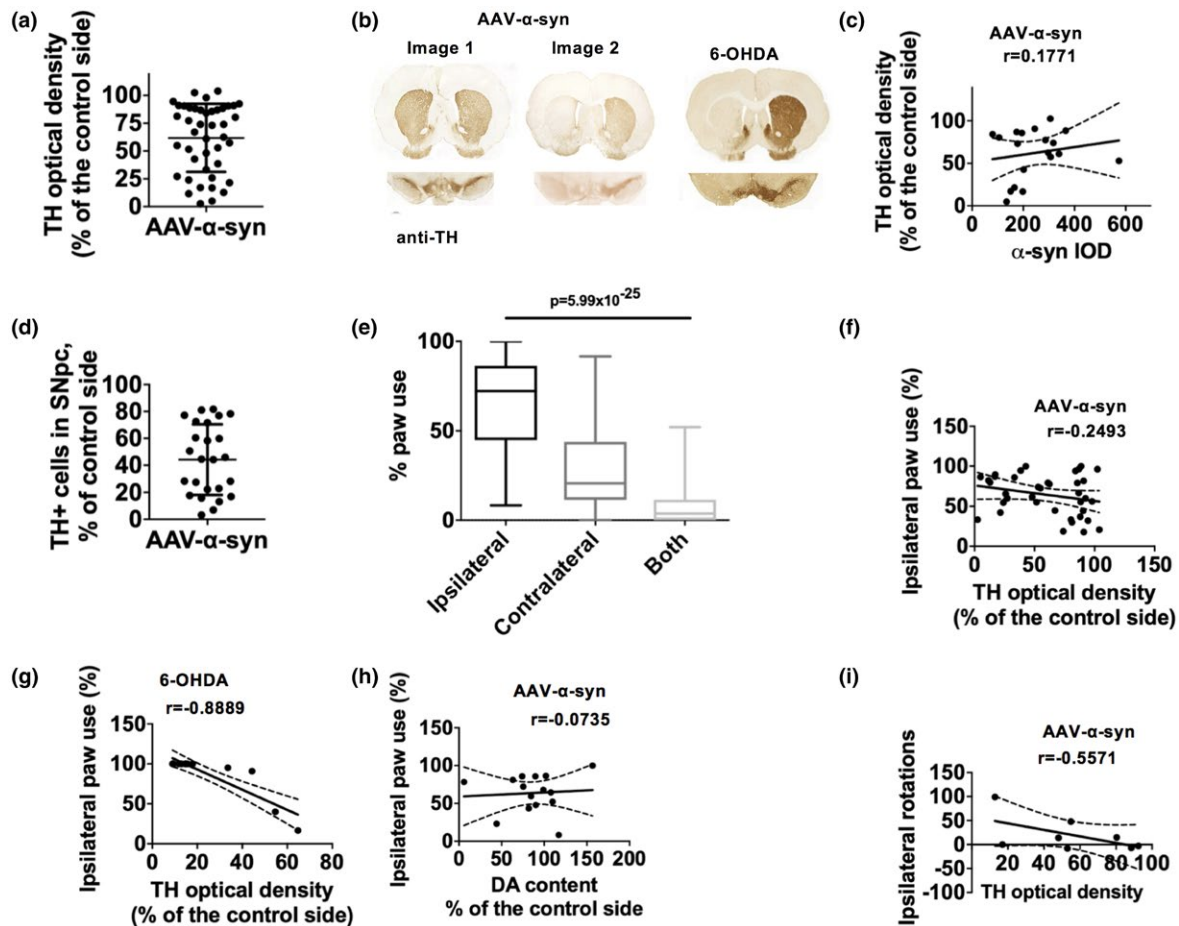


**FIGURE 2** There is a wide variation in nigrostriatal TH for AAV- $\alpha$ -synuclein injected rats that does not correlate with outcome measures. (a) Relative tyrosine hydroxylase (TH) optical density (percentage of the uninjected side) for AAV- $\alpha$ -synuclein (mixture of AAV2- $\alpha$ -synuclein and AAV5- $\alpha$ -synuclein, referred to as AAV- $\alpha$ -synuclein) injected rats 8 weeks after injection ( $n = 43$ ). (b) Photomicrographs of two example brains showing the striatum and substantia nigra injected with AAV- $\alpha$ -synuclein and one with 6-OHDA. (c) Correlation between relative TH optical density and  $\alpha$ -synuclein integrated optical density for AAV- $\alpha$ -synuclein injected rats. (d) TH+ cells in the substantia nigra as a percentage of the uninjected side for AAV- $\alpha$ -syn rats ( $n = 25$ ). (e) Cylinder test results for AAV- $\alpha$ -synuclein injected rats at 8 weeks after injection ( $n = 43$ ). Results are presented as ipsilateral, contralateral, and both paw touches as a percentage of total paw touches. (f) Correlation between ipsilateral paw use on the cylinder test and TH optical density for AAV- $\alpha$ -synuclein injected rats. (g) Correlation between ipsilateral paw use on the cylinder test and TH optical density for 6-OHDA injected rats. (h) Correlation between ipsilateral paw use on the cylinder test and dopamine content (as a percentage of the uninjected side) for AAV- $\alpha$ -synuclein injected rats. (i) Correlation between total rotations (ipsilateral–contralateral rotations) on the amphetamine-induced rotation assay (120 min) and TH optical density for AAV- $\alpha$ -synuclein injected rats.  $\pm$  SD is used for the error bar of graphs. All results are from 8 weeks post-AAV injection, female Sprague Dawley rats used

**TABLE 1** Summary of AAV2/2 and AAV2/5 mixture results and correlations

	TH optical density (OD) in STR	TH+ cells in SNpc (MATLAB)	TH+ cells in SNpc (Aiforia®)	Nissl+ cells (MATLAB)	Ipsilateral paw use (%)	Amphetamine-induced rotations
AAV- $\alpha$ -syn	61.85% $\pm$ 30.59%	44.25% $\pm$ 16.71%	58.51% $\pm$ 25.03%	81.41% $\pm$ 3.8%	66.04 $\pm$ 25.56	19.75 $\pm$ 36.89
AAV-eGFP	82.81% $\pm$ 34.03%	38.45% $\pm$ 21.92%	52.98% $\pm$ 22.08%	75.13% $\pm$ 12.8%	51.74 $\pm$ 22.3	38.71 $\pm$ 87.1
AAV-DIO-mCherry	92.57% $\pm$ 4.1%	51.18% $\pm$ 14.95%	67.34% $\pm$ 20.24%	73.53% $\pm$ 8.16%	46.03 $\pm$ 21.02	-2 $\pm$ 4.07
Correlations AAV- $\alpha$ -syn	TH OD - $\alpha$ -syn OD	TH OD-ipsilateral paw use			DA content-ipsilateral paw use	TH OD-amphetamine-induced rotations
Pearson's <i>r</i>	0.1771	-0.2493			0.0735	-0.5571

Note. Values are presented as percentages, percent of the control side,  $\pm$ SD.

**TABLE 2** The percentage of animals that are in each range of TH loss in the striatum for AAV- $\alpha$ -synuclein. *N* = 43

Percentage TH loss	Percentage of animals
0%-20%	39.5%
21%-40%	18.5%
41%-60%	14.0%
61%-80%	14.0%
81-100+%	14.0%

$r = -0.8889$ ,  $p = <0.0001$ ,  $n = 13$ ). As seen in this figure, all the animals with low TH optical density use the ipsilateral paw 100% of the time. We also measured dopamine content using HPLC and this also did not correlate with ipsilateral paw use (Figure 2h, Pearson's correlation  $r = 0.0735$ ,  $p = 0.7945$ ,  $n = 15$ ). Amphetamine-induced rotations were performed for selected animals and this showed a moderate correlation with TH optical density (Figure 2i, Pearson's correlation  $r = -0.5571$ ,  $p = 0.1515$ ,  $n = 8$ ). A summary of the results is shown in Table 1.

### 3.3 | Comparison of using AAV-eGFP and AAV-DIO-mCherry as controls for AAV- $\alpha$ -syn injections above substantia nigra

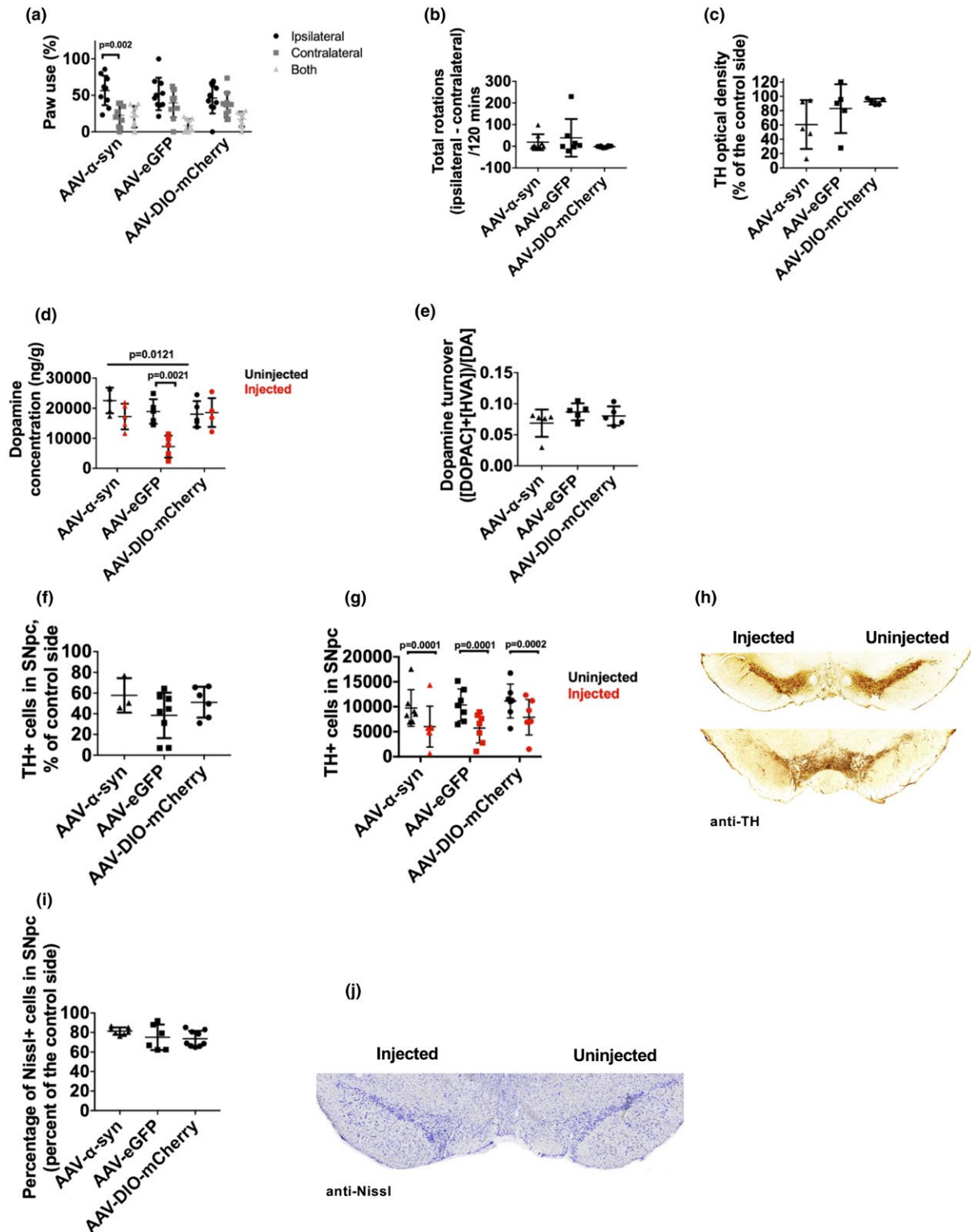
We next compared two controls in a single experiment using the same AAV- $\alpha$ -syn vectors as above, AAV-eGFP, and AAV-DIO-mCherry.

Due to the behavioral deficits and loss of TH we had observed with GFP overexpression from our initial experiments with AAV5 (Figure 1e,f), we also added another control vector of AAV-DIO-mCherry, in other words we tested two negative controls for AAV- $\alpha$ -syn. The DIO vector has an active promoter but does not produce any protein due to the inverted ORF (open reading frame). Additionally, the mixture of 2 and 5 serotypes were used to incur the advantage of the combination, and because we saw neurodegeneration with AAV5-eGFP (Figure 1e,f). We obtained similar results on cylinder behavior for AAV- $\alpha$ -syn as presented above (Figure 3a, two-way ANOVA, within-subjects factor paw use, between-subjects factor treatment; no significant interaction  $F(4, 54) = 1.67$ ,  $p = 0.1704$ ; no significant effect of treatment  $F(2, 27) = 1.636$ ,  $p = 0.2134$ ; significant effect of paw use  $F(2, 54) = 21.92$ ,  $p = <0.0001$ , Bonferroni post hoc test for multiple comparisons AAV- $\alpha$ -syn ipsilateral versus contralateral paw use adjusted  $p$  value = 0.002),  $n = 10$ /group). In this behavioral test, AAV-eGFP had no significant changes between ipsilateral and contralateral paw use (Figure 3a, post hoc test Tukey's multiple comparison for ipsilateral versus contralateral paw use adjusted  $p$  value = 0.4002). The AAV-DIO-mCherry group also had no behavioral deficits on cylinder test for ipsilateral versus contralateral paw use (Figure 3a, post hoc test Tukey's multiple comparison for ipsilateral versus contralateral paw use adjusted  $p$  value = 0.5833). However, the AAV-eGFP group had net positive ipsilateral rotations, though the mean was not significantly higher and there was large variation (Figure 3b, average rotations  $38.71 \pm 87.1$ ,  $n = 7$ ). Whereas,

**FIGURE 3** Comparing AAV- $\alpha$ -synuclein, AAV-eGFP, and AAV-DIO-mCherry in a single experiment. (a) Cylinder test results for AAV2 and AAV5 mixture vector injected rats at 8 weeks after injection. Results are represented as ipsilateral, contralateral, and both paw touches as a percentage of total paw touches. Both paw touches represents the number of times the animal placed both paws on the cylinder wall simultaneously.  $N = 10$ /group. (b) Total rotations (ipsilateral-contralateral) on the amphetamine-induced rotation assay (120 min) for all three AAV vector injected rats at 8 weeks. (c) Relative tyrosine hydroxylase (TH) optical density (percentage of the uninjected side) for AAV vector injected rats at 8 weeks post-injection. (d) Dopamine concentration (ng/g) for AAV vector injected rats at 8 weeks after AAV injection. Results are shown as both the total amount of dopamine measured for both the injected and uninjected side.  $N = 5$ /group. (e) Dopamine turnover for the injected side striatum. Calculated by summing the concentrations (ng/g) of 3,4-dihydroxyphenylacetic acid (DOPAC) and homovanillic acid (HVA) and dividing that by the concentration of dopamine (DA). (f) Percentage of TH+ cells in the substantia nigra pars compacta (percent of the uninjected side) for AAV vector injected rats at 8 weeks, analyzed using MATLAB. (g) Estimated number of TH+ cells in the substantia nigra pars compacta at 8 weeks post-AAV injection, analyzed using Aiforia®. (h) Representative images of TH staining in the substantia nigra at 8 weeks post-injection. (i) Percentage of Nissl+ cells in the substantia nigra pars compacta area (percent of the control side) for AAV vector rats at 8 weeks. (j) Representative image of Nissl-stained substantia nigra at 8 weeks post-injection.  $\pm$ SD is used for the error bar of graphs. Female Sprague Dawley rats used

the AAV-DIO-mCherry group had an average of approximately zero on net ipsilateral rotations (Figure 3b, average rotations  $-2 \pm 4.07$ ,  $n = 8$ ). For TH immunoreactivity, the results were variable and no significant differences were observed between the groups (Figure 3c, one-way ANOVA,  $F(2, 12) = 1.729$ ,  $p = 0.2188$ ,  $n = 5/\text{group}$ ), the average for the AAV- $\alpha$ -syn was similar to previous results. AAV- $\alpha$ -syn also showed a high variation similarly to the above-mentioned

results, also the SDs were similar (Figure 2a,  $SD = 30.59\%$ , Figure 3c,  $SD = 34.02\%$ ). The AAV-eGFP group did show a small drop in TH fiber density in the striatum (Figure 3c, average  $82.81\% \pm 34.03\%$ ), whereas the AAV-DIO-mCherry had a very modest drop (Figure 3c, average  $92.57\% \pm 4.1\%$ ). Dopamine concentration was also measured and there was a significant drop in dopamine concentration on the injected side compared to the uninjected side in the AAV-eGFP



group that was not observed in the other two groups, and this differed significantly from the AAV- $\alpha$ -syn group (Figure 3d, two-way ANOVA, within-subjects factor injection side, between-subjects factor treatment; significant interaction  $F(2, 12) = 5.54, p = 0.0198$ ; significant effect of treatment  $F(2, 12) = 6.553, p = 0.0119$ ; significant effect of injection  $F(1, 12) = 13.54, p = 0.0032$ ; Tukey's multiple comparison test for AAV-eGFP versus AAV- $\alpha$ -syn adjusted  $p$  value = 0.0121; Bonferroni's multiple comparison test uninjected versus injected side AAV-eGFP adjusted  $p$  value = 0.0021,  $n = 5$ /group). Dopamine turnover was calculated using the dopamine metabolites 3,4-dihydroxyphenylacetic acid (DOPAC) and homovanillic acid (HVA) as a ratio with the dopamine concentration (Figure 3e). This was calculated from the injected striatum for each rat. There were no significant differences between the three groups (One-way ANOVA,  $F(2, 12) = 1.406, p = 0.2828, n = 5$ /group). The TH+ cells in the substantia nigra pars compacta were analyzed using MATLAB and calculating the percentage compared to the control side (Figure 3f). Though there was clear cell loss, there were no significant differences between the groups (One-way ANOVA,  $F(2, 14) = 1.438, p = 0.6666, n = 3-8$ /group). Additionally, we performed a second method of analysis for TH+ cells using the Aiforia® platform which estimates the total number of TH+ cells in the substantia nigra pars compacta similarly to stereology. Each treatment group had a significant loss of TH+ cells in the substantia nigra pars compacta on the injected side; however, there were no differences between treatments (Figure 3g, two-way repeated measures ANOVA, within-subjects factor injection side, between-subjects factor treatment; no significant interaction  $F(2, 18) = 1.281, p = 0.3019$ ; no significant effect of treatment  $F(2, 18) = 0.4844, p = 0.6238$ ; significant effect of injection  $F(1, 18) = 117, p = <0.0001$ ; Bonferroni's multiple comparisons test for uninjected side versus injected side: AAV- $\alpha$ -syn adjusted  $p$  value =  $<0.0001$ , AAV-eGFP adjusted  $p$  value =  $<0.0001$ , AAV-DIO-mCherry adjusted  $p$  value = 0.0002,  $n = 7$ /group). Representative images of two TH-stained substantia nigras at different planes are shown in Figure 3h. The percentage of Nissl+ cells were analyzed (compared to the uninjected side) using cresyl violet staining in the substantia nigra pars compacta (Figure 3i). There were also no significant differences between the groups (One-way ANOVA,  $F(2, 19) = 1.675, p = 0.2139, n = 6-9$ /group). A representative image of a Nissl-stained substantia nigra is shown in Figure 3j. A summary of the results is shown in Table 1.

In addition to using AAV-eGFP and AAV-DIO-mCherry, we also used another non-protein-producing vector, the AAV1-DIO-iRFP, as well as a disabled vector where the promoter was replaced with lacZ (Figure 4). The AAV1-DIO-iRFP vector should only express protein in the presence of Cre recombinase. We also chose AAV1 vector to have another serotype to analyze whether similar results can be obtained with another kind of vector. These studies were performed to test other control vectors as well as ensure that any negative effects were not due to the virus but rather the transgene. A schematic for the pAAV-lacZ-DIO-iRFP (AAV1-lacZ-DIO) vector is shown in Figure 4a.

We found that transient transfections with pAAV-DIO-iRFP (AAV1-DIO-iRFP) vector showed robust expression in Cre+ cells, whereas the

pAAV-lacZ-DIO-iRFP (AAV1-lacZ-DIO) vector showed little to no expression; images without Cre are shown as a comparison (Figure 4b). The rats injected with AAV1-DIO-iRFP vector showed no behavioral deficits in cylinder test (Figure 4c, ipsilateral vs. contralateral paw use, one-way ANOVA,  $F(2, 69) = 12.07, p = 0.0875$ ), and the same results were obtained for the lacZ-DIO vector (Figure 4c, ipsilateral vs. contralateral paw use, one-way ANOVA,  $F(2, 27) = 1.102, p = 0.3467, n = 9-10$ /group). Some rats were rotating in the AAV1-lacZ-DIO-iRFP treatment group, there were no significant differences between the two groups (Figure 4d, unpaired  $t$ -test, two-tailed,  $t = 0.9505, df = 16, p = 0.3560, n = 9$ /group). While there was some variability in the results for TH optical density in both the AAV1-DIO-iRFP vector and the AAV1-lacZ-DIO-iRFP vector, there were no significant differences between the two (Figure 4e, unpaired  $t$  test, two-tailed,  $t = 0.4892, df = 16, p = 0.6314, n = 13$  for AAV1-DIO-iRFP and  $n = 5$  for AAV1-lacZ-DIO-iRFP). For the AAV1-DIO-iRFP vector, there was a mild correlation between ipsilateral paw use on the cylinder test and TH optical density (Figure 4f, Pearson's correlation,  $r = 0.4639, p = 0.1103$ ). This was similar for the AAV1-lacZ-DIO-iRFP vector correlation between TH optical density and ipsilateral paw use (Figure 4g, Pearson's correlation,  $r = 0.4453, p = 0.4523$ ). However, these correlations were the opposite of what was found in the 6-OHDA experiment (Figure 2g), and with both the vector alone or the vector with RNA expression the behavioral outcome is not similar to that of specific nigrostriatal degeneration. A summary of the results is found in Table 3.

## 4 | DISCUSSION

In the current studies, we set out to model Parkinson's disease using AAV to express large quantities of human wild-type  $\alpha$ -syn in the rat substantia nigra in order to have a model to test new therapeutics. The AAV- $\alpha$ -syn model is used in the field of Parkinson's animal models since it is thought that it more closely recapitulates the human disease than the toxin models (Yamada, Iwatsubo, Mizuno, & Mochizuki, 2004). However, while we were able to repeat what has been previously shown: approximately 40% loss of TH+ fiber density in the striatum (Febbraro et al., 2013) and moderate behavioral deficits on cylinder test (Decressac, Mattsson, Lundblad, Weikop, & Bjorklund, 2012), the results of TH loss in the striatum were highly variable and did not correlate with behavior. Therefore, expression of full-length human  $\alpha$ -syn may not be an optimal model to evaluate drug effects. In addition, we observed similar toxicities with GFP and  $\alpha$ -syn when the proteins were overexpressed in the substantia nigra using AAV viral vectors. To overcome the problem of GFP toxicity that occurred, we used vectors that expressed RNA that should not be translated, the AAV1-DIO-iRFP and AAV-DIO-mCherry vectors. In wild-type animals lacking Cre recombinase, this should not result in iRFP/mCherry RNA being translated to protein, and therefore no protein expression is taking place. Indeed, these RNA expressing control vectors showed little to no TH loss in the striatum and no behavioral deficits compared to AAV- $\alpha$ -syn and AAV-eGFP. This demonstrates the need for evaluating controls in these experiments.

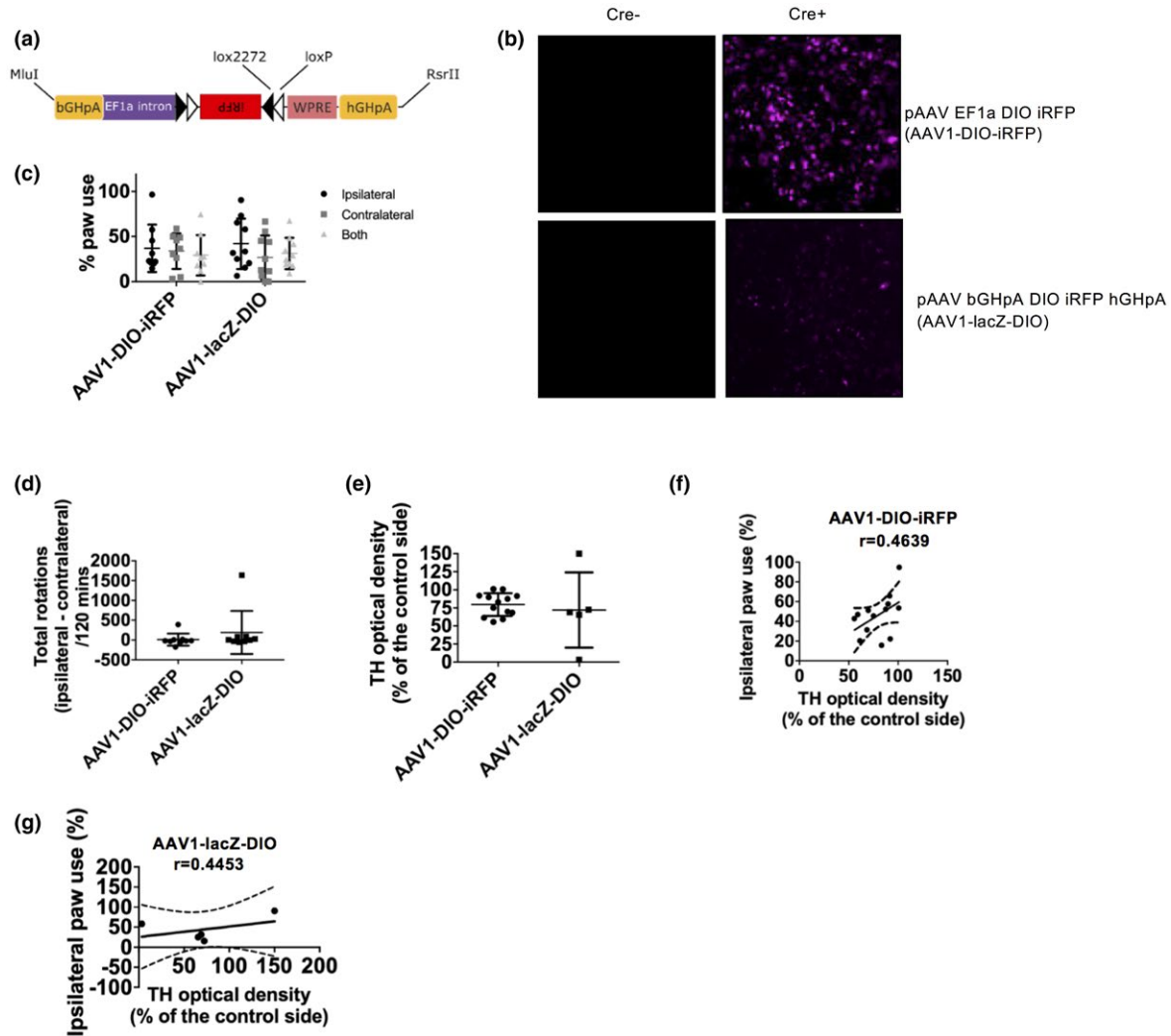


**FIGURE 4** Testing AAV1-DIO-iRFP and AAV1-lacZ-DIO as additional negative controls. (a) Schematic figure of AAV1-lacZ-DIO (pAAV-lacZ-DIO-iRFP). (b) Expression patterns of AAV1-DIO-iRFP and AAV1-lacZ-DIO vectors in cells without Cre (Cre-) and with Cre (Cre+). (c) Cylinder test results for AAV1-DIO-iRFP and AAV1-lacZ-DIO injected rats 8 weeks after injection ( $n = 10$ /group). Results are represented as ipsilateral, contralateral, and both paw touches as a percentage of total paw touches. (d) Total rotations (ipsilateral–contralateral) on the amphetamine-induced rotation assay (120 min) for AAV1-DIO-iRFP and AAV1-lacZ-DIO rats 8 weeks after injection.  $\pm$ SD is used for the error bar of graphs. (e) Relative tyrosine hydroxylase (TH) optical density (percentage of the uninjected side) for AAV1-DIO-iRFP and AAV1-lacZ-DIO injected rats 8 weeks after injection. (f) Correlation between ipsilateral paw use and TH optical density for AAV1-DIO-iRFP injected rats. (g) Correlation between ipsilateral paw use and TH optical density for AAV1-lacZ-DIO injected rats. Female Sprague Dawley rats used

**TABLE 3** AAV1 control summary results

	Ipsilateral paw use (%)	Amphetamine-induced rotations	TH OD in STR	Correlation: TH OD—ipsilateral paw use
AAV1-DIO-iRFP	36.92 $\pm$ 26.29	13.22 $\pm$ 151.9	79.58% $\pm$ 15.67%	0.4639
AAV1-lacZ-DIO	42.02 $\pm$ 27.99	191.9 $\pm$ 543.1	72.02% $\pm$ 52.11%	0.4453

Note. Values are presented as percentages, percent of the control side  $\pm$  SD. Correlation represented as Pearson's  $r$ .

Though  $\alpha$ -syn was present 8 weeks after the gene transfer in the substantia nigra and striatum and the animals showed preferential use of ipsilateral paw there was no statistically significant loss of striatal dopamine concentrations. In particular, it was clear that while some animals had a severe loss of TH in the striatum, many did

not. Thus, the decrease in contralateral paw use was clearly not due to degeneration of dopamine neurons in all rats, but rather reflected the loss of function of dopamine neurons. However, the specificity of the observed effects to  $\alpha$ -syn is questionable since we observed similar changes in TH and dopamine levels in GFP-injected animals.

Although we did observe a moderate correlation between TH optical density and amphetamine-induced ipsilateral rotations; however, it was not significant. Since the other outcome measures did not correlate it is unclear whether this would be a useful tool to evaluate the effectiveness of AAV- $\alpha$ -syn. Additionally, the AAV vectors seem to affect more the TH phenotype in the substantia nigra, since we do not see general cell loss with Nissl staining, nor loss of dopamine neurites or transmitter levels in the striatum with the DIO vectors. The number of TH<sup>+</sup> cells in the substantia nigra pars compacta was also analyzed using a similar method to stereology that uses a user-trained algorithm to recognize TH<sup>+</sup> cells (Penttinen, Parkkinen, Blom, et al., 2018). We performed this additional counting method to account for any changes that may occur on the contralateral side of the brain after AAV injection, as has been observed in the 6-OHDA model (Fox et al., 2016). We observed a significant drop in the injected side in all treatment groups indicating that the AAVs are downregulating TH in the substantia nigra and loss of TH with AAV-injection above substantia nigra does not reflect neurodegeneration. Moreover, caution needs to be exercised when using AAV-based transgene overexpression to model Parkinson's disease since a similar effect on TH downregulation has been observed with long-term overexpression of GDNF (glial cell line-derived neurotrophic factor) via AAV (Penttinen, Parkkinen, Voutilainen, et al., 2018).

Another factor to consider here in relation to the outcomes of this AAV model is that overexpression of  $\alpha$ -syn (or other proteins) may affect more than dopamine neurons of the substantia nigra. There are parvalbumin-expressing neurons present there (Gerfen, Baimbridge, & Miller, 1985) as well as other inhibitory GABAergic neurons (Lee & Tepper, 2007). Effects of  $\alpha$ -syn on these neurons directly may compromise their inhibitory actions by modulating GABA release, which may result in calcium increase at the synaptic level and in turn lead to neuronal loss (Mosharov et al., 2009). The role of GABA in Parkinson's disease is reviewed elsewhere (Błaszczyk, 2016). In the context of our current results, the potential effect of  $\alpha$ -syn on GABAergic inhibitory neurons and their synaptic transmission could result in no change in TH neurons but rather a dysfunction in, for example, cylinder behavior. This could therefore explain the lack of correlation between TH loss and behavior in these experiments.

When evaluating an animal model for human disease, researchers must always consider whether and how accurately it models the condition it purports to. While AAV- $\alpha$ -syn expression demonstrates better face validity than toxin models due to the presence of  $\alpha$ -syn, it may not be an accurate model of sporadic Parkinson's disease in humans. In human patients, SNCA ( $\alpha$ -syn encoding gene) mRNA is in fact decreased (Kingsbury et al., 2004). Whereas, unsurprisingly, overexpression of human  $\alpha$ -syn by AAV increases its protein levels in the rat brain (Decressac, Mattsson, Lundblad, et al., 2012). In a study that examined the effects of AAV- $\alpha$ -syn overexpression in rats in order to study the effects on GDNF and its related genes concluded that using AAV to overexpress human wild-type  $\alpha$ -syn in the rat substantia nigra is not a useful model for sporadic Parkinson's disease (Su et al., 2017).

It is possible that human  $\alpha$ -syn in rat brain decreases the likelihood of pathology compared to species-matching  $\alpha$ -syn, as has been observed in mouse models (Fares et al., 2016; Luk et al., 2016). Though when AAV- $\alpha$ -syn encoding the rat protein was injected to rat substantia nigra, there was actually less degeneration (Landeck et al., 2016). Related to this, it can be speculated that AAV- $\alpha$ -syn causes stronger degeneration of dopamine neurons in certain strains or species, as is the case with the toxin MPTP model (Jackson-Lewis & Przedborski, 2007); or that variation is lower depending on species, such as in the 6-OHDA model in rats, compared to mice where there is much higher variation between outcomes (Iancu, Mohapel, Brundin, & Paul, 2005). Moreover, it is also possible that the detrimental effects of control vectors may be different in different strains of mice and rats as well. Since Parkinson's disease is an aging-related disease, the age of animals may be an important factor in measuring outcomes in neurodegeneration studies based on proteinopathies such as  $\alpha$ -syn overexpression. It is known that older rats have less capacity to regrow damaged neurons compared to younger ones (Scheff & Scheff, 1979); therefore, it is becoming more pertinent to use aged rodents for Parkinson's disease models, and also aged nigrostriatal dopamine neurons may be more sensitive to stressors such as pathogenic proteins (Kanaan, Kordower, & Collier, 2008). Additionally, the time length of the experiment, 8 weeks, could have been a factor in TH loss, since while there was a functional effect, it may have taken longer to observe a more robust loss of TH across all animals. Also, at 8 weeks, enough potentially toxic aggregates may not be present in the brain to cause loss of TH neurons, such as in an AAV mouse study that only started to show Proteinase K-resistant  $\alpha$ -syn at 8 weeks (Svarcbahs, Julku, & Myohanen, 2016). However, several AAV- $\alpha$ -syn experiments have been conducted for 8 weeks or less and observed TH loss (Gombash et al., 2013; Gully et al., 2016), though how many animals showed the loss is less clear. Another potential contributor to the outcome of our study is the fact that unilateral, not bilateral, injections were used. In a study where the authors gave bilateral injections of AAV- $\alpha$ -syn to the substantia nigra pars compacta, they observed a significant loss of TH fibers in the striatum in comparison to GFP control and also number of TH neurons in the substantia nigra and ventral tegmental area at 8 weeks after the injection, as well as some behavioral changes (Caudal, Alvarsson, Bjorklund, & Svenningsson, 2015).

Since AAV-based vectors are currently in clinical trials for Parkinson's disease patients, we find it unlikely that the lesion was due to the AAV itself as it is considered safe to inject to the human brain (Bartus & Johnson, 2017). This of course could have been due to the mechanical damage during viral vector injection; however, we used glass capillaries that are considered to be less destructive in stereotaxic injections than steel needles (Gonzalez-Perez, Guerrero-Cazares, & Quinones-Hinojosa, 2010), and the needles were placed above the substantia nigra, not inside the structure. Also, from our experience with stereotaxic injections, we have found that thinner needles cause less mechanical damage. In addition to needle damage, injected volume may affect the outcome (Myers & Hoch, 1978). However, to control for the potential of the injection process or the

transgene itself to cause damage, we used a disabled vector which had the promoter replaced with lacZ. Since this showed low expression, even in the presence of Cre, we tested it in vivo and found that it had no significant effects on behavior, TH, or dopamine. This would indicate that it is not causing any unspecific damage in our experiments.

GFP toxicity has been reported previously (reviewed in (Albert et al., 2017)). It is clear that expressing a foreign protein in the mammalian brain may result in an immune response (Samaranch et al., 2014), and that overexpression of proteins can result in destruction of sensitive substantia nigra dopamine neurons (Klein et al., 2006), both of which can lead to unspecific neurodegeneration. It has been observed that injecting AAV-GFP above the substantia nigra at the same titer as AAV- $\alpha$ -syn also results in TH loss in the striatum (Andersen et al., 2018). And although this can be mitigated by lowering the titer of the AAV-GFP (Landeck et al., 2016), it may not be sound to do so when using it as a control to compare to another protein in disease models. In the case of overexpressing a disease-specific protein, the protein of interest should recapitulate the effects seen in the condition, and unspecific damage due to overexpressing a control protein at the same level should be considered problematic.

A general hypothesis is that dopamine neurons degenerate in a dying-back manner and the remaining neurons compensate by increasing striatal neurotransmission. In animal models of parkinsonism, it has been observed that there are compensatory adjustments and that nigrostriatal projections increase synthesis and release of dopamine (Calne & Zigmond, 1991; Snyder, Keller, & Zigmond, 1990). In the idiopathic parkinsonism, the neurological deficits do not appear until the loss of striatal dopamine is about 70% or more (Bernheimer, Birkmayer, Hornykiewicz, Jellinger, & Seitelberger, 1973) indicating increased dopamine neurotransmission to occur similarly as in animal models to compensate for the decrease in overall striatal dopamine concentrations. In line with this, *post mortem* analysis of dopamine metabolites suggests that there is increased dopamine turnover in Parkinson's disease patients (Hornykiewicz & Kish, 1987). Therefore, a possible future endeavor could be to use neuronal electrical activity and/or induced release of striatal dopamine as measurements of early degeneration in this or other  $\alpha$ -syn models.

From the varying TH loss and lack of correlation between cylinder test and  $\alpha$ -syn expression, it is apparent that we would need different measures to identify animals with dopamine degeneration. Ultrasonic vocalizations (Gombash et al., 2013), as well as motor tests related to gait (Caudal et al., 2015), such as the stepping test (Kirik et al., 2002), have been used as behavioral outcomes in the rat AAV- $\alpha$ -syn model. Alternatively, a way to measure changes in the dopamine system in a live animal could be used, for example, SPECT/CT technology, combining single-photon emission computed tomography and computed tomography, and radioligands for dopamine transporter as in (Back et al., 2013). This would be important to check whether an AAV- $\alpha$ -syn injection produced some deficit in

the dopamine system in order to properly model the disease and test potential therapeutics. A method to test the degree of neurodegeneration is important and could reduce the number of animals used in the long term. A study using AAV carrying the mutant form of  $\alpha$ -syn (A53T) was performed using PET and MRI to follow the time course of progression (Van der Perren et al., 2015), and therefore this technique could be used to check for successful effects on the dopamine system. However, outcome of the control injection still needs to be considered, and this would not solve the problems related to a mismatch between TH loss and behavioral outcome.

While overexpression of human wild-type  $\alpha$ -syn using AAV has been used successfully in several studies, for example (Bourdenx et al., 2015; Gorbatyuk et al., 2008), as well as overexpression of mutant forms of  $\alpha$ -syn as in (Klein, King, Hamby, & Meyer, 2002), these studies all use different serotypes, promoters, timelines, rat strains, and injection paradigms (reviewed in (Albert et al., 2017)). Here, except for one experiment that used male Wistar rats and a single injection above the substantia nigra using steel needles, the same settings were used for all the other experiments and we still observed variability. Therefore, while there is always going to be variability between animals, labs, and experiments, we would like to emphasize that careful consideration needs to be taken when carrying out these studies. As mentioned, we were able to, on average, repeat what has been published in the literature for this model (Decressac, Mattsson, Lundblad, et al., 2012; Febbraro et al., 2013; Gombash et al., 2013), but as can be seen from the large number of animals used there is high variability in the study, in regards to TH loss in particular. While this variability could be related to the viral vector itself, in other words the mixture of AAV2/2- $\alpha$ -syn and AAV2/5- $\alpha$ -syn, which was chosen to maximize efficacy, we still demonstrated similar results to already published studies: i.e. the average decrease in the TH optical density were almost identical as well as behavioral outcome on cylinder test. The issue remains that extensive preparation and testing needs to be undertaken before using this model for evaluation of drugs that may affect  $\alpha$ -syn and typical outcome measures used in Parkinson's animal models, especially when AAV is clearly downregulating TH in the substantia nigra in a non-specific manner. We found that vectors with DIO ORF that generate RNA were better controls than those with GFP because they showed less TH loss and no behavioral deficits, and we found similar effects with a vector that had a disabled promoter. However, as we have discussed earlier (Albert et al., 2017) a mammalian protein that forms non-toxic oligomers could be the more appropriate control to AAV- $\alpha$ -syn. This study demonstrates that AAV-mediated protein expression in large quantities can induce TH loss. Consequently, although high levels of wild-type  $\alpha$ -syn mimics Parkinson's pathology more closely, the observed effects may not mimic that in parkinsonian patients. Since this model gives highly variable results and it is clear that overexpression of AAV leads to TH downregulation caution needs to be taken with design of AAV-mediated studies, particularly with regards to disease models.

## DECLARATION OF TRANSPARENCY

The authors, reviewers and editors affirm that in accordance to the policies set by the Journal of Neuroscience Research, this manuscript presents an accurate and transparent account of the study being reported and that all critical details describing the methods and results are present.

## ACKNOWLEDGMENTS

We acknowledge Mart Saarma for initiating the studies and his input, insight, and encouragement throughout the experiments. We thank Timo Myöhänen for commenting on the manuscript. The materials and part of KA's salary was funded by Michael J. Fox Foundation for Parkinson's Research, and the other part KA's salary was funded by Finnish Parkinson's Foundation, Finnish Cultural Foundation, and the Ella and Georg Ehrnrooth Foundation. MHV was funded by Michael J. Fox Foundation for Parkinson's Research and by Academy of Finland grant #277910. MA was funded by Academy of Finland grant #250275. AD by Academy of Finland grant#293392. BKH and CR were funded by NIDA IRP.

## CONFLICTS OF INTEREST

The authors declare no conflict of interest.

## AUTHOR CONTRIBUTIONS

KA, MHV, MA, SA, and AD planned and carried out the experiments in vivo. BH developed the AAV1-DIO iRFP vector. CR developed, produced, and tested the AAV1-lacZ-DIO vector in vitro. KA and PP performed and analyzed the HPLC studies. KA together with MA wrote the paper. All authors commented on the manuscript.

## ORCID

Katrina Albert  <https://orcid.org/0000-0002-6129-4992>

Mikko Airavaara  <https://orcid.org/0000-0002-2026-1609>

## REFERENCES

- Airavaara, M., Mijatovic, J., Vihavainen, T., Piepponen, T. P., Saarma, M., & Ahtee, L. (2006). In heterozygous GDNF knockout mice the response of striatal dopaminergic system to acute morphine is altered. *Synapse*, 59(6), 321–329. <https://doi.org/10.1002/syn.20245>
- Albert, K., Voutilainen, M. H., Domanskyi, A., & Airavaara, M. (2017). AAV vector-mediated gene delivery to substantia nigra dopamine neurons: Implications for gene therapy and disease models. *Genes*, 8(63). <https://doi.org/10.3390/genes8020063>
- Alves, J. N., Muir, E. M., Andrews, M. R., Ward, A., Michelmore, N., Dasgupta, D., ... Rogers, J. H. (2014). AAV vector-mediated secretion of chondroitinase provides a sensitive tracer for axonal arborisations. *Journal of Neuroscience Methods*, 227, 107–120. <https://doi.org/10.1016/j.jneumeth.2014.02.010>
- Andersen, M. A., Christensen, K. V., Badolo, L., Smith, G. P., Jeggo, R., Jensen, P. H., ... Sotty, F. (2018). Parkinson's disease-like burst firing activity in subthalamic nucleus induced by AAV-alpha-synuclein is normalized by LRRK2 modulation. *Neurobiology of Diseases*, 116, 13–27. <https://doi.org/10.1016/j.nbd.2018.04.011>
- Back, S., Raki, M., Tuominen, R. K., Raasmaja, A., Bergstrom, K., & Mannisto, P. T. (2013). High correlation between in vivo [123I]beta-CIT SPECT/CT imaging and post-mortem immunohistochemical findings in the evaluation of lesions induced by 6-OHDA in rats. *EJNMMI Research*, 3(1), 46. <https://doi.org/10.1186/2191-219X-3-46>
- Bartus, R. T., & Johnson, E. M. Jr. (2017). Clinical tests of neurotrophic factors for human neurodegenerative diseases, part 1: Where have we been and what have we learned? *Neurobiology of Diseases*, 97(Pt B), 156–168. <https://doi.org/10.1016/j.nbd.2016.03.027>
- Bernheimer, H., Birkmayer, W., Hornykiewicz, O., Jellinger, K., & Seitelberger, F. (1973). Brain dopamine and the syndromes of Parkinson and Huntington. Clinical, morphological and neurochemical correlations. *Journal of the Neurological Sciences*, 20(4), 415–455.
- Blaszczyk, J. W. (2016). Parkinson's disease and neurodegeneration: GABA-collapse hypothesis. *Frontiers in Neuroscience*, 10, 269. <https://doi.org/10.3389/fnins.2016.00269>
- Blesa, J., & Przedborski, S. (2014). Parkinson's disease: Animal models and dopaminergic cell vulnerability. *Frontiers in Neuroanatomy*, 8, 155. <https://doi.org/10.3389/fnana.2014.00155>
- Bourdenx, M., Dovero, S., Engeln, M., Bido, S., Bastide, M. F., Duthiel, N., ... Dehay, B. (2015). Lack of additive role of ageing in nigrostriatal neurodegeneration triggered by alpha-synuclein overexpression. *Acta Neuropathologica Communications*, 3, 46. <https://doi.org/10.1186/s40478-015-0222-2>
- Braak, H., Del Tredici, K., Rub, U., de Vos, R. A., Jansen Steur, E. N., & Braak, E. (2003). Staging of brain pathology related to sporadic Parkinson's disease. *Neurobiology of Aging*, 24(2), 197–211. [https://doi.org/10.1016/S0197-4580\(02\)00065-9](https://doi.org/10.1016/S0197-4580(02)00065-9)
- Burre, J., Sharma, M., Tsetsenis, T., Buchman, V., Etherton, M. R., & Sudhof, T. C. (2010). Alpha-synuclein promotes SNARE-complex assembly in vivo and in vitro. *Science*, 329(5999), 1663–1667. <https://doi.org/10.1126/science.1195227>
- Calne, D. B., & Zigmond, M. J. (1991). Compensatory mechanisms in degenerative neurologic diseases. Insights from Parkinsonism. *Archives of Neurology*, 48(4), 361–363. <https://doi.org/10.1001/archneur.1991.00530160025009>
- Caudal, D., Alvarsson, A., Bjorklund, A., & Svenningsson, P. (2015). Depressive-like phenotype induced by AAV-mediated overexpression of human alpha-synuclein in midbrain dopaminergic neurons. *Experimental Neurology*, 273, 243–252. <https://doi.org/10.1016/j.expneurol.2015.09.002>
- Cheng, H. C., Ulane, C. M., & Burke, R. E. (2010). Clinical progression in Parkinson disease and the neurobiology of axons. *Annals of Neurology*, 67(6), 715–725. <https://doi.org/10.1002/ana.21995>
- Chu, Y., & Kordower, J. H. (2007). Age-associated increases of alpha-synuclein in monkeys and humans are associated with nigrostriatal dopamine depletion: Is this the target for Parkinson's disease? *Neurobiology of Diseases*, 25(1), 134–149. <https://doi.org/10.1016/j.nbd.2006.08.021>
- Davidson, B. L., Stein, C. S., Heth, J. A., Martins, I., Kotin, R. M., Derksen, T. A., ... Chiorini, J. A. (2000). Recombinant adeno-associated virus type 2, 4, and 5 vectors: Transduction of variant cell types and regions in the mammalian central nervous system. *Proceedings of the National Academy of Sciences of the United States of America*, 97(7), 3428–3432. <https://doi.org/10.1073/pnas.050581197>
- Decressac, M., Mattsson, B., & Bjorklund, A. (2012). Comparison of the behavioural and histological characteristics of the

- 6-OHDA and alpha-synuclein rat models of Parkinson's disease. *Experimental Neurology*, 235(1), 306–315. <https://doi.org/10.1016/j.expneurol.2012.02.012>
- Decressac, M., Mattsson, B., Lundblad, M., Weikop, P., & Bjorklund, A. (2012). Progressive neurodegenerative and behavioural changes induced by AAV-mediated overexpression of alpha-synuclein in mid-brain dopamine neurons. *Neurobiology of Diseases*, 45(3), 939–953. <https://doi.org/10.1016/j.nbd.2011.12.013>
- Fares, M. B., Maco, B., Oueslati, A., Rockenstein, E., Ninkina, N., Buchman, V. L., ... Lashuel, H. A. (2016). Induction of de novo alpha-synuclein fibrillization in a neuronal model for Parkinson's disease. *Proceedings of the National Academy of Sciences of the United States of America*, 113(7), E912–921. <https://doi.org/10.1073/pnas.1512876113>
- Febbraro, F., Sahin, G., Farran, A., Soares, S., Jensen, P. H., Kirik, D., & Romero-Ramos, M. (2013). Ser129D mutant alpha-synuclein induces earlier motor dysfunction while S129A results in distinctive pathology in a rat model of Parkinson's disease. *Neurobiology of Diseases*, 56, 47–58. <https://doi.org/10.1016/j.nbd.2013.03.014>
- Foundation, M. J. F. (2013). Update regarding MJFF & UNC-generated AAV viral vectors. Retrieved from <https://www.med.unc.edu/genetherapy/vectorcore/files/updateregardingmjffviralvectors-final>
- Fox, M. E., Mikhailova, M. A., Bass, C. E., Takmakov, P., Gainetdinov, R. R., Budygin, E. A., & Wightman, R. M. (2016). Cross-hemispheric dopamine projections have functional significance. *Proceedings of the National Academy of Sciences of the United States of America*, 113(25), 6985–6990. <https://doi.org/10.1073/pnas.1603629113>
- Gaugler, M. N., Genc, O., Bobela, W., Mohanna, S., Ardah, M. T., El-Agnaf, O. M., ... Schneider, B. L. (2012). Nigrostriatal overabundance of alpha-synuclein leads to decreased vesicle density and deficits in dopamine release that correlate with reduced motor activity. *Acta Neuropathologica*, 123(5), 653–669. <https://doi.org/10.1007/s00401-012-0963-y>
- Gerfen, C. R., Baimbridge, K. G., & Miller, J. J. (1985). The neostriatal mosaic: Compartmental distribution of calcium-binding protein and parvalbumin in the basal ganglia of the rat and monkey. *Proceedings of the National Academy of Sciences of the United States of America*, 82(24), 8780–8784. <https://doi.org/10.1073/pnas.82.24.8780>
- Giasson, B. I., Jakes, R., Goedert, M., Duda, J. E., Leight, S., Trojanowski, J. Q., & Lee, V. M. (2000). A panel of epitope-specific antibodies detects protein domains distributed throughout human alpha-synuclein in Lewy bodies of Parkinson's disease. *Journal of Neuroscience Research*, 59(4), 528–533. [https://doi.org/10.1002/\(SICI\)1097-4547\(20000215\)59:4<528:AID-JNR8>3.0.CO;2-0](https://doi.org/10.1002/(SICI)1097-4547(20000215)59:4<528:AID-JNR8>3.0.CO;2-0)
- Gombash, S. E., Manfredsson, F. P., Kemp, C. J., Kuhn, N. C., Fleming, S. M., Egan, A. E., ... Sortwell, C. E. (2013). Morphological and behavioral impact of AAV2/5-mediated overexpression of human wild-type alpha-synuclein in the rat nigrostriatal system. *PLoS ONE*, 8(11), e81426. <https://doi.org/10.1371/journal.pone.0081426>
- Gonzalez-Perez, O., Guerrero-Cazares, H., & Quinones-Hinojosa, A. (2010). Targeting of deep brain structures with microinjections for delivery of drugs, viral vectors, or cell transplants. *Journal of Visualized Experiments*, (46). <https://doi.org/10.3791/2082>
- Gorbatyuk, O. S., Li, S., Sullivan, L. F., Chen, W., Kondrikova, G., Manfredsson, F. P., ... Muzyczka, N. (2008). The phosphorylation state of Ser-129 in human alpha-synuclein determines neurodegeneration in a rat model of Parkinson disease. *Proceedings of the National Academy of Sciences of the United States of America*, 105(2), 763–768. <https://doi.org/10.1073/pnas.0711053105>
- Gully, J. C., Sergeev, V. G., Bhootada, Y., Mendez-Gomez, H., Meyers, C. A., Zolotukhin, S., ... Gorbatyuk, O. S. (2016). Up-regulation of activating transcription factor 4 induces severe loss of dopamine nigral neurons in a rat model of Parkinson's disease. *Neuroscience Letters*, 627, 36–41. <https://doi.org/10.1016/j.neulet.2016.05.039>
- Henderson, M. J., Wires, E. S., Trychta, K. A., Richie, C. T., & Harvey, B. K. (2014). SERCaMP: A carboxy-terminal protein modification that enables monitoring of ER calcium homeostasis. *Molecular Biology of the Cell*, 25(18), 2828–2839. <https://doi.org/10.1091/mbc.E14-06-1141>
- Hornykiewicz, O., & Kish, S. J. (1987). Biochemical pathophysiology of Parkinson's disease. *Advances in Neurology*, 45, 19–34.
- Howard, D. B., Powers, K., Wang, Y., & Harvey, B. K. (2008). Tropism and toxicity of adeno-associated viral vector serotypes 1, 2, 5, 6, 7, 8, and 9 in rat neurons and glia in vitro. *Virology*, 372(1), 24–34. <https://doi.org/10.1016/j.virol.2007.10.007>
- Iancu, R., Mohapel, P., Brundin, P., & Paul, G. (2005). Behavioral characterization of a unilateral 6-OHDA-lesion model of Parkinson's disease in mice. *Behavioral Brain Research*, 162(1), 1–10. <https://doi.org/10.1016/j.bbr.2005.02.023>
- Jackson-Lewis, V., & Przedborski, S. (2007). Protocol for the MPTP mouse model of Parkinson's disease. *Nature Protocols*, 2(1), 141–151. <https://doi.org/10.1038/nprot.2006.342>
- Kanaan, N. M., Kordower, J. H., & Collier, T. J. (2008). Age-related changes in dopamine transporters and accumulation of 3-nitrotyrosine in rhesus monkey midbrain dopamine neurons: Relevance in selective neuronal vulnerability to degeneration. *European Journal of Neuroscience*, 27(12), 3205–3215. <https://doi.org/10.1111/j.1460-9568.2008.06307.x>
- Kankaanpaa, A., Meririnne, E., Ariniemi, K., & Seppala, T. (2001). Oxalic acid stabilizes dopamine, serotonin, and their metabolites in automated liquid chromatography with electrochemical detection. *Journal of Chromatography B: Biomedical Sciences and Applications*, 753(2), 413–419. [https://doi.org/10.1016/S0378-4347\(00\)00553-3](https://doi.org/10.1016/S0378-4347(00)00553-3)
- Kingsbury, A. E., Daniel, S. E., Sangha, H., Eisen, S., Lees, A. J., & Foster, O. J. (2004). Alteration in alpha-synuclein mRNA expression in Parkinson's disease. *Movement Disorders*, 19(2), 162–170. <https://doi.org/10.1002/mds.10683>
- Kirik, D., Rosenblad, C., Burger, C., Lundberg, C., Johansen, T. E., Muzyczka, N., ... Bjorklund, A. (2002). Parkinson-like neurodegeneration induced by targeted overexpression of alpha-synuclein in the nigrostriatal system. *Journal of Neuroscience*, 22(7), 2780–2791. <https://doi.org/10.1523/JNEUROSCI.2002-02.2002>
- Klein, R. L., Dayton, R. D., Leidenheimer, N. J., Jansen, K., Golde, T. E., & Zweig, R. M. (2006). Efficient neuronal gene transfer with AAV8 leads to neurotoxic levels of tau or green fluorescent proteins. *Molecular Therapy*, 13(3), 517–527. <https://doi.org/10.1016/j.ymthe.2005.10.008>
- Klein, R. L., King, M. A., Hamby, M. E., & Meyer, E. M. (2002). Dopaminergic cell loss induced by human A30P alpha-synuclein gene transfer to the rat substantia nigra. *Human Gene Therapy*, 13(5), 605–612. <https://doi.org/10.1089/10430340252837206>
- Landeck, N., Buck, K., & Kirik, D. (2016). Toxic effects of human and rodent variants of alpha-synuclein in vivo. *European Journal of Neuroscience*, 1–12. <https://doi.org/10.1111/ejn.13493>
- Lee, C. R., & Tepper, J. M. (2007). Morphological and physiological properties of parvalbumin- and calretinin-containing gamma-aminobutyric acid neurons in the substantia nigra. *The Journal of Comparative Neurology*, 500(5), 958–972. <https://doi.org/10.1002/cne.21220>
- Lindholm, P., Voutilainen, M. H., Lauren, J., Peranen, J., Leppanen, V. M., Andressoo, J. O., ... Saarna, M. (2007). Novel neurotrophic factor CDNF protects and rescues midbrain dopamine neurons in vivo. *Nature*, 448(7149), 73–77. <https://doi.org/10.1038/nature05957>
- Luk, K. C., Covell, D. J., Kehm, V. M., Zhang, B., Song, I. Y., Byrne, M. D., ... Lee, V. M. (2016). Molecular and biological compatibility with host alpha-synuclein influences fibril pathogenicity. *Cell Reports*, 16(12), 3373–3387. <https://doi.org/10.1016/j.celrep.2016.08.053>
- Matlik, K., Vihinen, H., Bienemann, A., Palgi, J., Voutilainen, M. H., Booms, S., ... Arumae, U. (2017). Intrastrially infused exogenous

- CDFN is endocytosed and retrogradely transported to substantia nigra. *eNeuro*, 4(1). <https://doi.org/10.1523/ENEURO.0128-16.2017>
- Mosharov, E. V., Larsen, K. E., Kanter, E., Phillips, K. A., Wilson, K., Schmitz, Y., ... Sulzer, D. (2009). Interplay between cytosolic dopamine, calcium, and alpha-synuclein causes selective death of substantia nigra neurons. *Neuron*, 62(2), 218–229. <https://doi.org/10.1016/j.neuron.2009.01.033>
- Myers, R. D., & Hoch, D. B. (1978). 14C-dopamine microinjected into the brain-stem of the rat: Dispersion kinetics, site content and functional dose. *Brain Research Bulletin*, 3(6), 601–609. [https://doi.org/10.1016/0361-9230\(78\)90006-0](https://doi.org/10.1016/0361-9230(78)90006-0)
- Penttinen, A. M., Suleymanova, I., Albert, K., Anttila, J., Voutilainen, M. H., & Airavaara, M. (2016). Characterization of a new low-dose 6-hydroxydopamine model of Parkinson's disease in rat. *Journal of Neuroscience Research*, 94(4), 318–328. <https://doi.org/10.1002/jnr.23708>
- Penttinen, A. M., Parkkinen, I., Blom, S., Kopra, J., Andressoo, J. O., Pitkanen, K., ... Airavaara, M. (2018). Implementation of deep neural networks to count dopamine neurons in substantia nigra. *European Journal of Neuroscience*, 48(6), 2354–2361. <https://doi.org/10.1111/ejn.14129>
- Penttinen, A. M., Parkkinen, I., Voutilainen, M. H., Koskela, M., Back, S., Their, A., ... Airavaara, M. (2018). Pre-alpha-pro-GDNF and Pre-beta-pro-GDNF isoforms are neuroprotective in the 6-hydroxydopamine rat model of Parkinson's disease. *Frontiers in Neurology*, 9, 457. <https://doi.org/10.3389/fneur.2018.00457>
- Samaranch, L., San Sebastian, W., Kells, A. P., Salegio, E. A., Heller, G., Bringas, J. R., ... Bankiewicz, K. S. (2014). AAV9-mediated expression of a non-self protein in nonhuman primate central nervous system triggers widespread neuroinflammation driven by antigen-presenting cell transduction. *Molecular Therapy*, 22(2), 329–337. <https://doi.org/10.1038/mt.2013.266>
- Schallert, T., Fleming, S. M., Leasure, J. L., Tillerson, J. L., & Bland, S. T. (2000). CNS plasticity and assessment of forelimb sensorimotor outcome in unilateral rat models of stroke, cortical ablation, Parkinsonism and spinal cord injury. *Neuropharmacology*, 39(5), 777–787. [https://doi.org/10.1016/S0028-3908\(00\)00005-8](https://doi.org/10.1016/S0028-3908(00)00005-8)
- Scheff, S. W., & Scheff, S. W. (1979). Compensatory synapse growth in aged animals after neuronal death. *Mechanisms of Ageing and Development*, 9(1–2), 103–117.
- Snyder, G. L., Keller, R. W. Jr, & Zigmond, M. J. (1990). Dopamine efflux from striatal slices after intracerebral 6-hydroxydopamine: Evidence for compensatory hyperactivity of residual terminals. *The Journal of Pharmacology and Experimental Therapeutics*, 253(2), 867–876.
- Spillantini, M. G., Schmidt, M. L., Lee, V. M., Trojanowski, J. Q., Jakes, R., & Goedert, M. (1997). Alpha-synuclein in Lewy bodies. *Nature*, 388(6645), 839–840. <https://doi.org/10.1038/42166>
- Su, X., Fischer, D. L., Li, X., Bankiewicz, K., Sortwell, C. E., & Federoff, H. J. (2017). Alpha-synuclein mRNA is not increased in sporadic PD and alpha-synuclein accumulation does not block GDNF signaling in Parkinson's disease and disease models. *Molecular Therapy*, 25(10), 2231–2235. <https://doi.org/10.1016/j.ymthe.2017.04.018>
- Svarcbahs, R., Julku, U. H., & Myohanen, T. T. (2016). Inhibition of prolyl oligopeptidase restores spontaneous motor behavior in the alpha-synuclein virus vector-based parkinson's disease mouse model by decreasing alpha-synuclein oligomeric species in mouse brain. *Journal of Neuroscience*, 36(49), 12485–12497. <https://doi.org/10.1523/JNEUROSCI.2309-16.2016>
- Van der Perren, A., Toelen, J., Casteels, C., Macchi, F., Van Rompuy, A. S., Sarre, S., ... Baekelandt, V. (2015). Longitudinal follow-up and characterization of a robust rat model for Parkinson's disease based on overexpression of alpha-synuclein with adeno-associated viral vectors. *Neurobiology of Aging*, 36(3), 1543–1558. <https://doi.org/10.1016/j.neurobiolaging.2014.11.015>
- Yamada, M., Iwatsubo, T., Mizuno, Y., & Mochizuki, H. (2004). Overexpression of alpha-synuclein in rat substantia nigra results in loss of dopaminergic neurons, phosphorylation of alpha-synuclein and activation of caspase-9: Resemblance to pathogenetic changes in Parkinson's disease. *Journal of Neurochemistry*, 91(2), 451–461. <https://doi.org/10.1111/j.1471-4159.2004.02728.x>

## SUPPORTING INFORMATION

Additional supporting information may be found online in the Supporting Information section at the end of the article.

Transparent Science Questionnaire for Authors.

**How to cite this article:** Albert K, Voutilainen MH, Domanskyi A, et al. Downregulation of tyrosine hydroxylase phenotype after AAV injection above substantia nigra: Caution in experimental models of Parkinson's disease. *J Neuro Res*. 2018;00:1–16. <https://doi.org/10.1002/jnr.24363>